

AURORA SYNCHRONIZATION IMPROVEMENT

D. M. Weidenheimer, N. R. Pereira, and D. C. Judy*
 Berkeley Research Associates, Inc.,
 PO Box 852, Springfield, VA 22150-0852

* Harry Diamond Laboratories, Adelphi, MD, 20783-1197

Abstract:

The Aurora flash x-ray simulator has undergone a series of hardware upgrades over the past five years. The upgrades have improved simulator reliability and have provided new environments for hardness testing.

Recently, synchronization of the four pulse-forming lines (PFLs) has been significantly improved over the original design. The four parallel PFLs are now synchronized to within 10 ns over 60% of the shots. This paper describes the current switching scheme, reports the current timing statistics, and discusses the effects of improved synchronization on hardness test parameters such as shot to shot reproducibility of the dose.

1. INTRODUCTION

Aurora^{1,2}, a 14 TW flash gamma-ray simulator operated by Harry Diamond Laboratories for the Defense Nuclear Agency since 1972, was designed to provide four individual radiation pulses that overlap to give a single 120 ns wide pulse for TREE testing. Recently, Aurora has become suitable as a tactical SREMP simulator thanks to the 7-ns risetime of a single radiation pulse achieved with a gas erosion cell,³ and to the 30 ns pulse width obtained by energy diversion.⁴ However, to get the desired radiation levels, all four pulses must overlay within 10 ns. On a recent shot series of 31 shots the mean time difference between the first and last pulse (window) was slightly less than 10ns. This paper describes the configuration used for 10 ns synchronization. An alternate approach was presented at an earlier conference.⁵

Figure 1 shows Aurora's pulse power system. The driver is a 14 MV Marx generator that consists of four parallel 1.25 MJ units connected together to drive four parallel oil-dielectric Blumlein pulse-forming lines (PFLs). Each PFL is coupled to an E-beam diode via a magnetically insulated transmission line (MITL).

The desired synchronization is achieved, in part, by symmetrizing the four Blumleins as much as possible, including the physical connection to the Marx generator. The dashed lines in figure 1 symbolize the original connections with the Marx. The solid lines indicate a single-node connection scheme that equalizes the pulse charge of the Blumleins. However, the principal improvement comes from redesigning the gas switch that triggers the four 12 MV oil Blumlein switches.

Figure 2 shows the Blumlein switching region. The oil switch is a V/N type with its trigger electrode discharged through an externally triggered gas switch. The original gas switch was a two-stage V/N switch that needed an additional self-break gap called the Trigger Isolation Gap (TIG). The jitter (standard deviation) of this switch, including the TIG, was about 6.5 ns. The new switch is a single-stage trigatron with a measured jitter of 1.5 ns.

2. DIAGNOSTICS & MEASUREMENTS

The principal voltage sensors in all four PFLs are located as indicated in figures 1 and 2. Figure 3 contains typical pulse shapes and corresponding timing characteristics. After the initial trigger signal to the Marxes, the voltage on the intermediate conductor of each 22 Ω Blumlein (figure 3a) increases

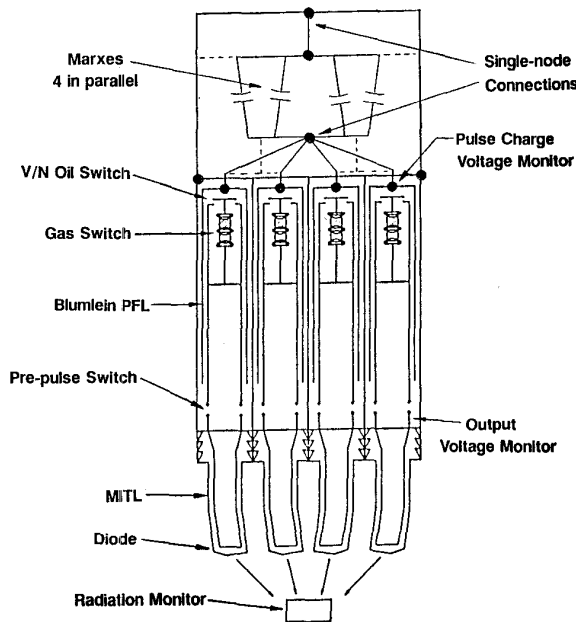


Figure 1. Block diagram of the Aurora system. The solid lines between Marx and Blumleins schematically indicate their connections (at "single-node connections"), the dashed lines suggest the original connection scheme.

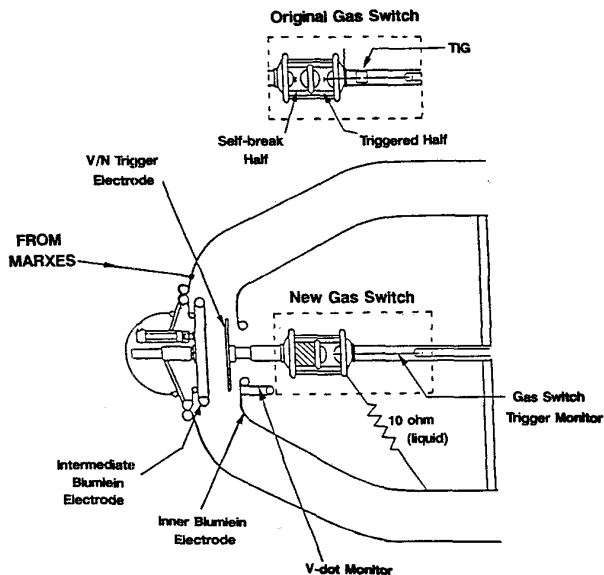


Figure 2. Aurora Blumlein switching region. The original two-stage gas V/N switch with Trigger Isolation Gap (TIG) is given in the insert.

toward a -9 MV peak in approximately $1.8 \mu\text{s}$. When the voltage has reached a preset level, here -3 MV, a single trigger generator sends a $\sim +75$ kV pulse through four 375 ns long $50\text{-}\Omega$ cables to each gas switch (figure 3b). The trigatron gas switch closes in about 25 ns. This discharges the oil trigger electrode capacitance through its support structure. Figure 3c is the voltage on the oil trigger electrode measured by integrating the signal from the V-dot probe indicated in figure 2.

A sudden change in voltage on the trigger electrode initiates closure of the trigger electrode to the intermediate electrode. Closure occurs in about 140 ns (but inversely proportional with voltage.) After the trigger electrode has discharged to the intermediate, the gap between the trigger and inner electrode breaks down (in about 20 ns) and the oil switch is closed.

Oil switch closure launches the pulse in the Blumlein PFL. When the pulse reaches the output end of the line, after 65 ns, the prepulse switch breaks down (in about 30 ns) and the pulse proceeds to the MITL and the diode. Total system runtime is the time interval between the gas switch trigger generator pulse and the output voltage exceeding 5 MV (see figure 3d).

Much effort has been spent on measuring, maintaining and calibrating signal cables and sensors to attain ~ 2 ns timing accuracy for each of the signals. Hewlett-Packard Model 54112D digitizing oscilloscopes are used for waveform recording and initial analysis of data. Additional timing measurements are made with Racal Dana Model 1991 time interval meters that have 1 ns resolution. System runtimes and runtimes of the individual elements are measured with the internal cursors of the digitizing oscilloscopes. The resolution in the amplitude measurement is about 3% .

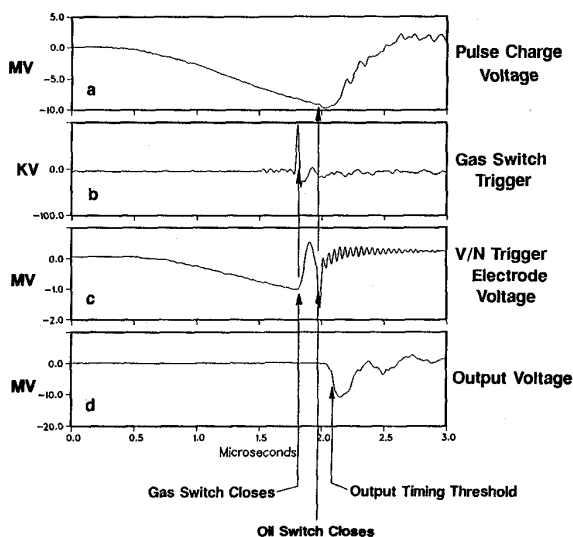


Figure 3. Measurements of a typical switching sequence. a. PFL charging voltage; b. the gas switch trigger; c. voltage on the oil switch trigger electrode; d. output pulse voltage, with timing threshold.

3. TOWARD 10 ns SYNCHRONIZATION

3.1 Equalizing Pulse Charging

All elements in the switching chain are affected by the pulse charge voltage. In particular, the closure time t_c of the oil switch is approximately⁵

$$t_c \approx t_{1c} \left[\frac{E_{av}}{1\text{MV/cm}} \right]^\alpha,$$

where $E_{av} = V/d$ is the average electric field from a voltage V across an oil gap with width d , $t_{1c} \approx 22$ ns is the closure time for an average electric field of 1 MV/cm, and the exponent α is approximately 1.3 . A relative difference in voltage $\Delta V/V$ then translates into a relative difference in closing time t_c of

$$\Delta t_c/t_c \sim -\alpha \Delta V/V.$$

Synchronization, therefore, demands symmetric pulse charging of all four Blumleins.

The necessary symmetry could not be obtained with the machine configured for multi-pulse operation⁷ because the paired Marxes exhibited different and variable timing characteristics. The variability of the Marx banks can be sidestepped, in part, by connecting the Marxes together into one single pulser. In addition, all four Marx banks are charged from the same power supply and triggered with a common trigger. Further improvement results from connecting the Marx banks to the PFLs only at two single nodes, one at the high-voltage end and one at the low-voltage end. This configuration implies increased inductance in the connections between Marx and PFLs, resulting in a ~ 100 ns (5%) increase in pulse-charge time.

3.2 Trigatron gas switch

The ~ 0.75 m² area trigger electrode (figure 2) is capacitively balanced between the -9 MV peak intermediate Blumlein electrode at a distance of ~ 5 cm from the (ground) inner electrode. During pulse charging the ~ 250 pF trigger electrode capacitance charges up with ~ 0.25 mC to about -1 MV. Discharging the trigger electrode through the gas switch disturbs the capacitive balance of the trigger electrode. The sudden large electric field at the sharpened edge of the trigger electrode is thought to initiate discharges in the oil⁶. Once started, the discharges develop into arcs that eventually close the oil switch.

It was difficult to trigger the original two-stage V/N gas switch (see insert in figure 2) with accuracy because closure of this gas switch demanded three separate gaseous discharges, each with their individual jitter characteristics. The first was the trigger isolation gap (TIG). This TIG allowed the gas switch trigger electrode to float electrically during the pulse charge, the same function that the gas switch has for the oil switch trigger electrode. The TIG's jitter was measured at 3 ns⁹. The second discharge was the triggered section of the gas switch, with a jitter of 2 ns⁹. Moreover, the jitter in the discharge of the gas switch self-break section was about 6 ns⁹.

The gas switch presently implemented in Aurora is a single-stage trigatron¹⁰ built mostly with old hardware from the original switch. The self-break section was bypassed by replacing the insulator with a conductor. The insulator in the triggered section was grooved on the inside to help prevent surface flashover, and the insulator length was increased to keep the average field strength between electrodes below 250 kV/cm. The trigger pin is connected directly to the $+75$ kV pulse from the trigger generator. The jitter of this trigatron as installed in the machine is 1.5 ns (over 88 shots).

3.3 Oil Switch Experimentation

The trigger electrode in the oil switch is azimuthally sym-

metric. Therefore, discharges can start at any position on the trigger electrode edge. The number of arcs affects the discharge time of the oil switch because the number of spark channels N determines the oil switch inductance L . For N channels of radius ρ equispaced on a circle of radius r ,

$$L = \frac{\mu_0 \ell}{2\pi} \left[\frac{1}{N} \ln \frac{R}{N\rho} + \frac{N-1}{N} \ln \frac{R}{r} \right].$$

Here R is the radius of the return conductor, and ℓ is the length of the current channels. For Aurora $R \sim 2$ m, $\ell \sim 0.5$ m, $r \sim 0.5$ m, while the channel radius ρ is unknown. Taking $\rho \sim 1$ cm for a definite example, the inductance varies by a factor ~ 4 between a single channel $N = 1$ and $N \geq 4$.

The number of arcs can be limited⁶ by rounding the trigger electrode, and providing sharp inserts. We tested this concept for a series of shots on Aurora. With three inserts, the risetime of the output pulse increases, but the risetime does not become more reproducible. Instead, on an occasional shot the risetime increases substantially, apparently when the oil switch contains fewer than three arc channels. Direct optical evidence was not obtained because the arcs were not directly observable. Moreover, the inserts were heavily damaged after only a few shots, even when refractory materials such as elconite, tantalum, or tungsten (which shatters) were used. Therefore, this approach was abandoned.

The increase in output pulse risetime realized when using three inserts, as compared with that achieved using a standard sharpened trigger electrode, suggests that many discharge channels contribute to switch closure when using a sharp electrode. Experimentation with various electrode spacings confirms that the optimum position for the trigger electrode (5 cm) maintains electrostatic equilibrium with the unperturbed potential distribution between inner and intermediate electrodes.⁸ This electrode spacing has been used for all shots reported in this paper.

Erosion of the sharpened trigger electrode, when operated at 5 cm spacing, occurs rather uniformly around its circumference. This normal wear does not seem to affect arc initiation, perhaps because charge injection from the sharpest points modifies the local electric field. Self-closing of the oil switch occurs very rarely and seems to be the only source of severe, localized damage to the electrode edge.

Damage to the trigger electrode edge could conceivably be avoided by keeping arcs away from the trigger electrode. This might be done by reducing the trigger electrode radius so that it is smaller than the inner electrode aperture. In a test series of a few shots with a trigger electrode of 0.3 m radius (reduced from 0.5 m), we were able to trigger the oil switch. Arcs apparently bypassed the trigger electrode, because its voltage did not show the large negative spike seen in figure 3d. Unfortunately, a mechanical problem unrelated to trigger electrode size prevented a comprehensive assessment of the triggering accuracy, although damage to the electrode edge after a few shots was minimal.

Adding a 10 Ω resistance between the ground electrode of the gas switch and the inner Blumlein skin (see figure 2) damps late-time oscillations in the trigger circuit and may reduce trigger electrode wear. This resistance bypasses the inductive support structure and consequently decreases the trigger voltage risetime on the oil trigger electrode (the half-period decreases from ~ 100 ns to ~ 75 ns). Without a quantitative measure for damage to the trigger electrode it is hard to say exactly how much the resistance reduces electrode damage. This 10 Ω resistance remains in place for all shots reported in this paper.

The jitter in the oil switch runtime is the largest remaining contributor to system runtime jitter. Measured jitter of the oil switches was 5.7 ns over 88 shots. The cause of the remaining variability in the oil switch run time is unclear. Runtime variations seem consistent with differences in pulse charge voltages on the different PFLs. Unfortunately, the estimated 3% accuracy of the voltage measurement is insufficient to show correlations between runtime and voltage. We are presently contemplating a measurement of the difference in pulse charge voltages from the current induced in a pipe with inductance L between two of the return current conductors. Besides giving ΔV from $\Delta V = LdI/dt$ the current I in this connection should further equalize the pulse charge voltages, and improve synchronization. Arc initiation in oil appears to be reproducible^{5,6} to within our measurement error.

4. SYNCHRONIZATION RESULTS

Figure 4 illustrates the synchronization achieved between the four Blumleins for the 31 shots immediately after implementing the single-point Marx connection and the trigatron gas switch. The figure gives the time difference between the first and the last output pulse, i.e., the time window that contains all four pulses. The most frequently occurring window is about 8 ns. The probability distribution around this mode is approximately Gaussian, with 21 of 31 shots (68%) at 10 ns or less. On the 4 shots where the window exceeded 15 ns, an anomaly could be identified and corrected for the next shot. For a series of 95 shots, the mode goes to 10 ns with 60% of total shots at 10 ns or less.

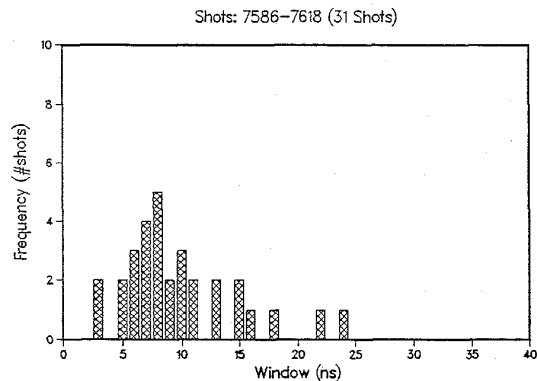


Figure 4. The number of shots as function of the time difference between first and last pulse, the timing window for 31 shots.

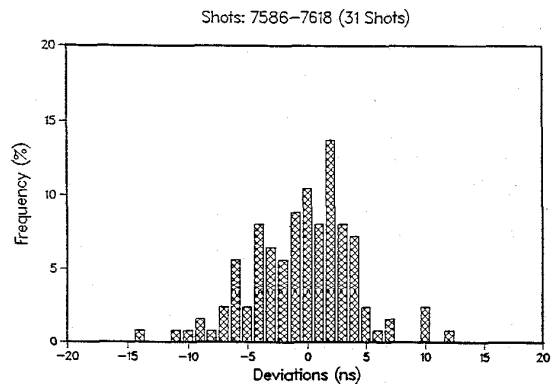


Figure 5. The distribution of the runtimes of the individual pulse forming lines (with respect to the average runtime on the same shot) for 31 shots.

Figure 5 shows the probability distribution for the runtimes of the individual Blumleins relative to the average runtime on a given shot. The standard deviation in this distribution is a reasonable measure of the jitter between the four PFLs. The 31 shots shown in figure 5 yielded a jitter of 4.3 ns. The jitter only increases to 4.4 ns for a larger series of 95 shots.

5. SHOT TO SHOT REPRODUCIBILITY

Although the primary purpose of this work is improved synchronization between the four Blumleins on a single shot, an important benefit is improved shot to shot reproducibility of the bremsstrahlung pulse. In the original design, the trigger pulse for Blumlein triggering was delayed by a fixed time after triggering of the Marx. Shot to shot variations in Marx erection then influence the pulse charge voltage waveform and magnitude at the time the Blumlein triggers. In turn, this voltage influences output pulse amplitude and timing. The influence of Marx variability on output voltage is avoided, in part, by a voltage-controlled Blumlein trigger generator. The voltage-controlled trigger improves the shot to shot reproducibility of output voltage and ultimately, bremsstrahlung radiation. However, triggering must be initiated about 800 ns before the Blumlein discharge, allowing some shot to shot variation from the Marx to be transmitted to the pulse charge.

It is possible to measure the dose from the individual diodes using lead collimators in line with the centerline of each diode looking toward the diode surface. Figure 6 shows the dose from the individual diodes plotted against the dose ~ 1 m away from all four diodes on the centerline of the machine. On shots where the four Marx banks erect synchronously, the dose produced by the individual diodes is identical to within the $\sim 3\%$ standard deviation. On these shots the total dose at 1 m is reproducible to within 2.2%. The best shot, with a dose of ~ 6150 rad(Si), at 1 m shows the smallest difference between individual diodes.

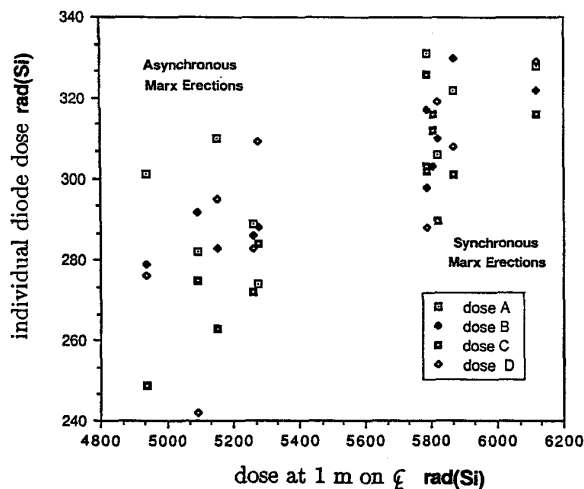


Figure 6. The dose from each individual diode plotted against the total dose of the four overlapping radiation pulses at 1 m away from the machine on the centerline.

However, when the Marx banks do not erect simultaneously the dose at 1 m is more than 10% smaller, and the difference between shots is larger. Obviously, the dose of the individual diodes is also smaller, but in addition, the difference between the doses from individual diodes has increased. On all 11 shots, the low-voltage end of the Marx was connected

at two different points to the Blumleins, which makes it possible for irregularities in Marx erection to show up as differences between Blumleins.

6. IMPROVEMENTS IN PROGRESS

Although the synchronization requirements have been met, we continue to implement various improvements suggested by the research. The most beneficial is to improve the reliability of the Marx erections. Simultaneous and reproducible erection ensures close to the same pulse charge voltage on the Blumleins, and equal voltage waveforms and radiation output from the diodes. Other ways of equalizing the pulse charge voltages will also be explored. Finally, we will increase the rate of rise dV/dt of the voltage on the trigger electrode by decreasing circuit capacitance and inductance. The inductance can be reduced by shunting the inductive support structure with falsework etc., and the capacitance will be reduced by decreasing the trigger electrode radius.

Acknowledgements

It is a pleasure to thank D. Lindsay and J. Deaver for their help in the Marx modifications, S. G. Gorbics for the dosimetry, and J. Ramirez, D. L. Johnson, and B. Turman of Sandia National Labs, for their consultation. This work was supported by the Defense Nuclear Agency and the Harry Diamond Laboratories.

References

- [1] I. Smith and B. Bernstein, "Aurora, An electron accelerator," IEEE Trans. on Nucl. Sci. NS-20, pp294-300 (1973).
- [2] F. J. Agee, "New capabilities of the Aurora flash x-ray machine," review talk given at the 1990 International Conference on Applications of Accelerators in Research and Industry, Denton, TX, 1990 (to be published in Nucl. Instr. Meth., 1991).
- [3] G. Merkel, HDL, private communication
- [4] K. Nielsen, "Aurora Upgrade Vol 4 - Divertor Switch Pulse Shortening," Pulse Sciences, Inc. report to DNA, contract: DNA001-85-C-0140.
- [5] F. T. Warren, H. G. Hammon, B. N. Turman, and K. R. Prestwich, "Jitter Improvement on the 12 MV Oil Switches on Aurora," Proc. 5th IEEE Pulsed Power Conference, Arlington, VA, (1985), edited by P. J. Turchi and M. F. Rose.
- [6] N. R. Pereira, D. M. Weidenheimer and J. Golden, "The 12 MV oil switch on Aurora," to be submitted to J. Appl. Phys., 1991.
- [7] K. Nielsen, "Aurora Upgrade I: - Multipulse Modification and Tests," Pulse Sciences, Inc. report to DNA, contract: DNA001-85-C-140.
- [8] "Phase II Final Report, Aurora Simulator Development Program," Vol. II, "The Aurora Diode Experiment (ADE)," Physics International Co. report to DNA, contract: DASA 01-68-c-0175 (1968).
- [9] D. M. Weidenheimer et al., "Jitter reduction on Aurora," internal BRA report (1990).
- [10] P. E. Peterkin and P. F. Williams, "Triggering in trigatron spark gaps: a fundamental study," J. Appl. Phys. 66, 4163 (1989); see also T. H. Martin, "Pulse charged gas breakdown," Proc. 5th IEEE Pulsed Power Conference, Arlington, VA, (1985), edited by P. J. Turchi and M. F. Rose.